1080 *J. Phys. Chem.* **1994**, *98*, 1080–1086

Iminopropadienones, RN=C=C=C=O: Theory and Experiment

Thomas Mosandl, Stefan Stadtmüller, Ming Wah Wong,* and Curt Wentrup*

Chemistry Department, The University of Queensland, Brisbane, Queensland 4072, Australia

Received: October 11, 1993; In Final Form: November 11, 1993⊗

Ab initio molecular orbital calculations at the MP2/6-31G* level have been used to examine the structures and infrared spectra of a new class of compounds, the iminopropadienones, RN=C=C=C=O (R = H, CH_3, and Ph). The agreement between calculated and experimental IR spectra of PhNCCCO, $Ph^{15}NCCCO$, and $PhNCC^{13}CO$ is excellent. Inclusion of electron correlation is found to be important for the correct prediction of the relative intensities of the cumulenic stretching vibrations. All three iminopropadienones are predicted to have a slightly bent NCCCO backbone (∠CCC ≈ 176°). As with carbon suboxide, these cumulenes are calculated to have an extremely flat CCC bending potential. The parent compound, HNCCCO (**4a**) is calculated to be thermodynamically stable toward dissociations into (i) HNCC + CO, (ii) HNC + CCO, (iii) HN + CCCO, and (iv) $H^\bullet$ + $NCCCO^\bullet$. Rearrangement of **4a** to the more stable cyanoketene isomer requires a sizeable barrier of 402 kJ mol^{-1} [G2(MP2)]. The calculated stability of **4a** is consistent with its experimental observation in neutralization–reionization mass spectrum. The adiabatic ionization energy and heat of formation of HNCCCO are predicted to be 9.51 eV and 175 kJ mol^{-1}, respectively.

1. Introduction

The first experimental evidence for the existence of iminopropadienones, RN=C=C=C=O (**4**), was reported recently.[1] The phenyl derivative **4c** was obtained from three different precursors (**1–3**) in flash vacuum pyrolysis (FVP) reactions, whereby **1** and **2** gave particularly good yields (Scheme 1). **4c** was characterized by chemical trapping reactions. Both the methyl (**4b**) and phenyl (**4c**) derivatives have been observed by IR[1] and mass spectrometry,[2] and the unsubstituted compound, HN=C=C=C=O (**4a**), has been produced by dissociative ionization of methyl 5-aminoisoxazole-4-carboxylate in a tandem mass spectrometer and characterized by neutralization–reionization mass spectrometry.[2] Further work on the characterization of the related bisimines, RN=C=C=C=NR′, is currently in progress.[3] All these compounds can be considered as imines of carbon suboxide, O=C=C=C=O, a reactive but isolable molecule.[4]

In this paper, we report high-level ab initio theoretical calculations on the structures and infrared spectra of these cumulenes. ^{15}N- and ^{13}C-labeled isotopomers of the phenyl derivative (**4c**) have been generated, and their IR spectra are in excellent agreement with the theoretical predictions. In addition, we have examined the stability with respect to rearrangement and fragmentation, ionization energy and thermochemistry for the parent compound, HN=C=C=C=O (**4a**).

2. Theory

Method and Results. Standard ab initio molecular orbital calculations[5] were carried out with the GAUSSIAN 92 series of programs.[6] Geometry optimizations for **4a–c** were carried out with the split-valence polarized 6-31G* basis set[5] at the Hartree–Fock (HF) and second-order Møller–Plesset perturbation (MP2) levels.[5] Harmonic vibrational wavenumbers and infrared intensities were predicted at these equilibrium geometries using analytical second derivatives.[7] The directly calculated HF/6-31G* wavenumbers were scaled by a factor of 0.89 to account for the overestimation of vibrational wavenumbers at this level of theory.[8] For the unsubstituted iminopropadienone (**4a**) and related species, higher-level energy calculations were computed using the Gaussian-2 [G2(MP2)] theory,[9] which is a composite procedure based effectively on QCISD(T)/6-311+G(3df,2p)//MP2/6-31G* energies together with zero-point vibrational and isogyric corrections. Unless otherwise noted, these are the values referred to in the text. To investigate the bending potential function of HNC_3O (**4a**), we have carried out geometry optimizations at the HF and MP2 levels for a number of bent structures corresponding to various values of the CCC angle. These were performed with the 6-31G* basis set. Spin-restricted calculations were used for closed shell systems and spin-unrestricted for open-shell systems. The frozen-core approximation was employed for all correlation calculations.

SCHEME 1

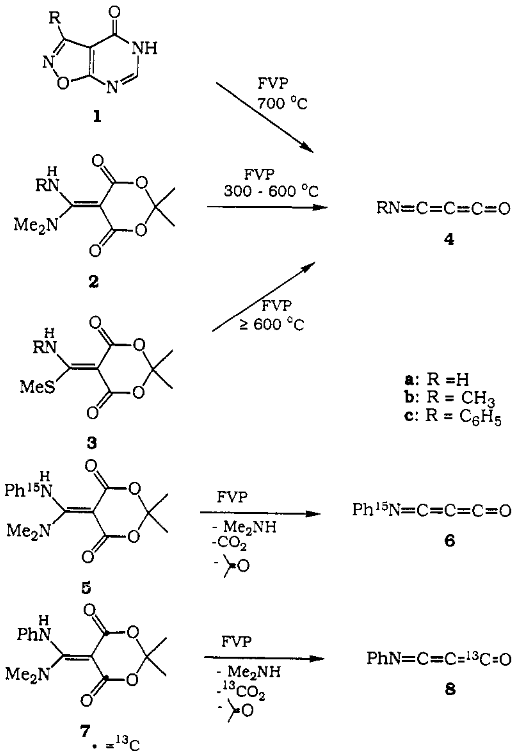

The results of geometry optimizations for the iminopropadienones (**4a–c**) are summarized in Tables 1 and 2. Figure 1 displays the planar (**4a**) and nonplanar, bent (**4a′**) structures of HNC_3O.

⊗ Abstract published in *Advance ACS Abstracts*, December 15, 1993.

0022-3654/94/2098-1080$04.50/0

TABLE 1: Optimized Structural Parameters for Iminopropadienones (RN=C=C=C=O)[a]

	HF/6-31G*			MP2/6-31G*		
parameter[b]	R = H	R = CH_3	R = C_6H_5	R = H	R = CH_3	R = C_6H_5
r(R–N)	0.996	1.420	1.382	1.011	1.437	1.390
$r(N–C_1)$	1.192	1.156	1.161	1.222	1.213	1.218
$r(C_1–C_2)$	1.275	1.296	1.291	1.287	1.292	1.288
$r(C_2–C_3)$	1.264	1.253	1.256	1.278	1.276	1.278
$r(C_3–O)$	1.146	1.155	1.153	1.188	1.192	1.190
$\angle RNC_1$	127.9	179.9	179.9	131.0	144.0	144.6
$\angle NC_1C_2$	175.1	180.0	180.0	171.4	172.7	173.2
$\angle C_1C_2C_3$	179.3	179.8	180.0	175.6	175.7	177.0
$\angle C_2C_3O$	179.9	180.0	180.0	179.6	179.5	179.6
τRNC_1C_2	180.0	176.5	176.9	180.0	179.4	178.4
$\tau NC_1C_2C_3$	177.1	174.2	168.1	180.0	179.5	179.8
$\tau OC_3C_2C_1$	5.6	178.5	177.2	180.0	177.2	170.1

[a] Bond lengths are given in angstroms and bond angles in degrees. [b] Atom labels are illustrated in Figure 1.

TABLE 2: Calculated Structural Parameters[a] and Rotational Constants[b] for HNC_3O (4a)[a]

parameter	MP2/ 6-31+G(2d)	MP2/ 6-311+G(2df,2p)	QCISD(T)/ 6-31G*
	Geometry		
r(H–N)	1.012	1.004	1.015
$r(N–C_1)$	1.217	1.210	1.228
$r(C_1–C_2)$	1.288	1.281	1.290
$r(C_2–C_3)$	1.280	1.274	1.281
$r(C_3–O)$	1.180	1.174	1.188
$\angle HNC_1$	132.1	133.3	125.8
$\angle NC_1C_2$	172.4	173.2	171.3
$\angle C_1C_2C_3$	177.9	178.9	174.2
$\angle C_2C_3O$	179.9	180.0	179.4
τHNC_1C_2	180.0	180.0	178.5
$\tau NC_1C_2C_3$	179.9	179.7	163.5
$\tau OC_3C_2C_1$	179.8	179.2	179.9
	Rotational Constants		
A	1070.41	1133.02	814.61
B	2.1568	2.1783	2.1471
C	2.1524	2.1741	2.1416

[a] Bond lengths are given in angstroms and bond angles in degrees. [b] In gigahertz.

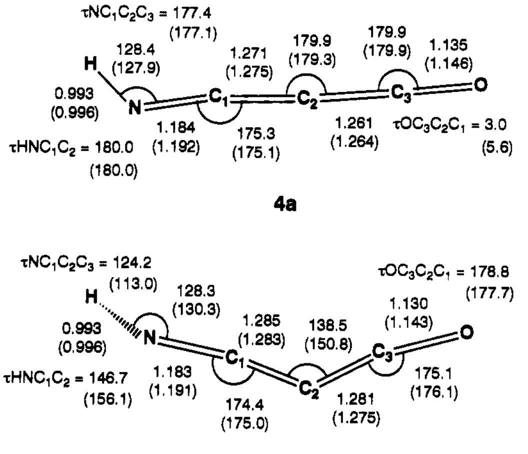

4a

4a'

Figure 1. Optimized geometries (HF/6-311+G(2df,2p), with HF/6-31G* values in parentheses) of planar (**4a**) and bent (**4a′**) structures of HNC_3O.

Calculated bending potential functions for HNC_3O is presented in Figure 2. Calculated charges (MP2/6-31G*), based on natural bond orbital (NBO) analysis,[10] of the iminopropadienones are given in Table 3. The G2(MP2) total and relative energies of **4a** and related species are given in Table 4. Optimized MP2/6-31G* structures for cyanoketene (**9**), transition structure for the rearrangement of **4a** to **9** (**10**) and iminopropadienone radical cation ($HNC_3O^{•+}$, **11**) are shown in Figure 3. Vibrational wavenumbers and infrared intensities of the iminopropadienones and their ^{15}N and ^{13}C isotopomers are presented in Table 5. The normal vibrations calculated for HNC_3O at the MP2/6-31G* level are illustrated in Figure 4. Comparison of MP2/3-21G and MP2/6-31G* cumulenicic stretching wavenumbers and IR intensities are given in Table 6. Finally, comparison of calculated and experimental cumulenic CO stretching wavenumbers are summarized in Table 7.

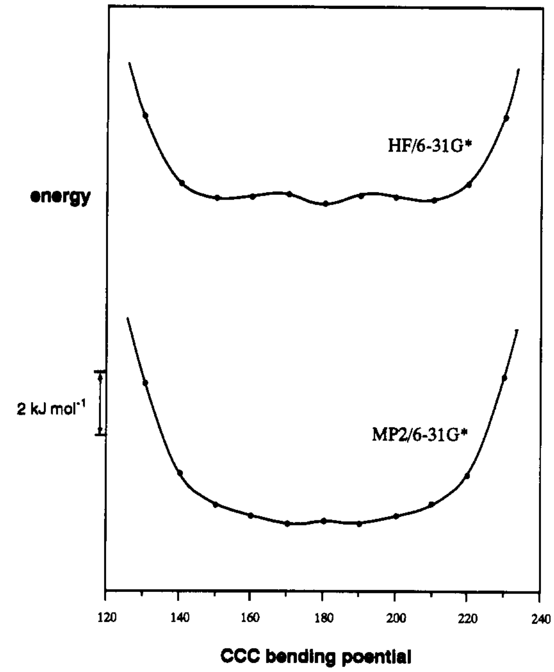

Figure 2. Calculated bending potential functions for HNC_3O.

TABLE 3: Calculated NBO Charges of Iminopropadienones (RN=C=C=C=O)[a]

atom[b]	R = H (**4a**)	R = CH_3 (**4b**)	R = Ph (**4c**)
R	0.435	0.252	0.203
N	–0.613	–0.381	–0.374
C_1	0.440	0.434	0.438
C_2	–0.482	–0.484	–0.463
C_3	0.629	0.607	0.611
O	–0.408	–0.428	–0.415

[a] MP2/6-31G* wave function. [b] Atom labels are illustrated in Figure 1.

TABLE 4: Calculated Total Energies[a] (hartrees) and Relative Energies[a] (kJ mol^{-1}) of HNC_3O (4a) and Related Species

species	state	sym	total energy	rel energy
HNCCCO (**4a**)	$^1A'$	C_s	–244.448 67	0.0
HNCCCO	$1\Sigma^+$	$C_{\infty v}$	–244.443 51	13.5
NCCHCO (**9**)	$^1A'$	C_s	–244.474 71	–68.4
TS: **4a** → **9** (**10**)	^1A	C_1	–244.295 55	402.0
$HNCCCO^{•+}$ (**11**)	2A″	C_s	–244.099 08	917.9
$HNCCCO^{•+}$ [b]	2A″	C_s	–244.090 82	939.5
$HCCN(^1A') + CO(^1\Sigma^+)$			–244.361 52	228.8
$HNCC(^1A') + CO(^1\Sigma^+)$			–244.322 95	330.1
$H^•(^2S) + NCCCO^•(^2\Pi)$			–243.311 13	361.1
$HNC(^1\Sigma^+) + CCO(^1\Sigma^+)$[c]			–244.273 00	461.2
$HN(^1\Sigma^+) + CCCO(^1\Sigma^+)$			–244.188 73	682.5

[a] G2(MP2) E_0 energies. [b] Corresponding to vertical ionization of HNC_3O. [c] Note that the lowest-energy singlet state of C_2O corresponds to a $^1\Delta$ state. The energy difference between $^1\Sigma^+$ and $^1\Delta$ states is 25.5 kJ mol^{-1} (complex MP2/6-31G*).

Equilibrium Structures of RNC_3O. To the best of our knowledge, there is no theoretical calculation reported on the structures of the iminopropadienones. The parent species, HNC_3O (**4a**), is an isoelectronic analogue of carbon suboxide (O=C=C=C=O), of which the spectra have been studied extensively in the millimeter-wave, far-infrared, mid-infrared, and ultraviolet regions.[4] Strong experimental evidence has

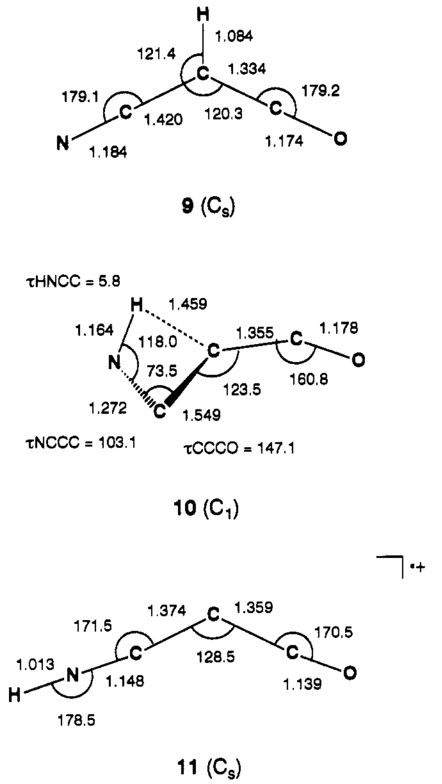

Figure 3. Optimized geometries (MP2/6-31G*) of cyanoketene (**9**), transition structure for the rearrangement of **4a** to **9** (**10**), and $HNC_3O^{•+}$ radical cation (**11**).

indicated that C_3O_2 is a semirigid bender, with a central CCC bond angle of 156°.[4b,c] Thus, the molecular structures of the iminopropadienones are of considerable interest in terms of their bending potentials.

To investigate the possible conformations of iminopropadienone, geometry optimizations for HNC_3O (**4a**) were carried out systematically with a sequence of basis sets, namely, 3-21G, 6-31G*, 6-311G*, 6-31+G*, 6-31G(2d), 6-31G(df), and 6-311+G(2df,2p) basis sets,[8] at the Hartree–Fock level. The effect of electron correlation was investigated at the MP2[5] and QCISD(T)[11] levels, using the 6-31G* basis set. The calculated structure of HNC_3O is very sensitive to the theoretical level employed. With the smallest basis set, 3-21G, there is only one stable equilibrium structure, with a linear HNCCCO framework. At the HF/6-31G* level, there exists two stable conformations, the planar, essentially linear (**4a**) and the nonplanar, bent (**4a′**) structures (Figure 1). Both structures have almost identical energy. The central CCC bond angle of the bent structure (**4a′**) is 151°, similar to that of C_3O_2.[4b,c] Both conformations are true local minima (with all real frequencies) on the HNC_3O potential energy surface. Expansion of the basis set from double-ζ valence to triple-ζ valence (6-31G* → 6-311G*) and inclusion of f functions on heavy atoms (6-31G* → 6-31G(df)) have little effect on the structures and relative energies of **4a** and **4a′**. Inclusion of diffuse sp functions on heavy atoms (6-31G* → 6-31+G*) favors the "planar" structure. In fact, at this level of theory (HF/6-31+G*), the "planar" structure (**4a**) is the only stable equilibrium structure of HNC_3O. On the other hand, expansion of the basis set from one set of d-polarization functions to two (6-31G* → 6-31G(2d)) strongly favors the bent structure (**4a′**), with a significant increase of the degree of bending (∠CCC = 132°). **4a′** is the only stable HNCCCO structure at the HF/6-31G(2d) level. With the largest 6-311+G(2df,2p) basis set, both **4a** and **4a′** exist and the energy difference between the conformations is just 3 kJ mol^{-1}, in favor of the bent structure. Inclusion of electron correlation at the MP2 level strongly favors the "planar" conformation. No stable bent conformation of HNC_3O (**4a′**) was found at the MP2/6-31G* level. This is confirmed by a larger-basis-set [6-31+G(2d)] optimization at the MP2 level (Table 2). To establish a more definitive theoretical estimate of the molecular structure of the cumulene, we have carried out geometry optimizations of **4a** and **4a′** at the MP2/6-311+G(2df,2p) and QCISD(T)/6-31G* levels (Table 2). As with the MP2/6-31G* and MP2/6-31+G(2d) levels, the "planar" structure (**4a**) is the only stable form of HNCCCO. In other words, the improvement of basis set [6-31+G(2d) → 6-311+G(2df,2p)] as well as higher-level treatment of electron correlation [QCISD(T)] favor the "planar" structure. This result lends confidence to our prediction of the molecular structures of the iminopropadienones at the MP2/6-31G* level. Calculated rotational constants of **4a** are given in Table 2.

Geometry optimizations were carried out for all three derivatives of iminopropadienones (**4a–c**) with the 6-31G* basis set at both the Hartree–Fock and MP2 levels (Table 1). At the HF level, the iminopropadienones are predicted to be essentially planar, with almost linear CCC angles. However, inclusion of electron correlation (MP2) increases significantly the degree of bending for all three derivatives (by 3–4°). A similar finding has been reported for the structurally related species, propadienone ($CH_2{=}C{=}C{=}O$).[12] It is worthwhile to note that the calculated structural parameters for propadienone[10a] at the MP2/6-31G* level agree well with experimental values.[13] At the MP2/6-31G* level, the iminopropadienones are predicted to be have a slightly bent NCCCO framework (∠CCC = 176–177°). For the parent compound (**4a**), we have examined the CCC bending potential functions, obtained by optimizing a number of bent structures, with a range of CCC angles, at both the HF/6-31G* and MP2/6-31G* levels. The result (Figure 3) clearly indicates that *the CCC bending potential is extremely flat.* Constraining the HNCCCO skeleton to be linear (i.e., $^1\Sigma^+$ state) increases the energy by 14 kJ mol^{-1} (Table 4). Thus, the calculated barrier to completely linearity is 14 kJ mol^{-1}. This result suggests that the HNC bending potential is significantly steeper than the CCC curve. A similar finding has been reported for the quasi-linear molecule HNCO.[14] In summary, the iminopropadienones are best considered as quasi-linear molecules.

Interestingly, all three iminopropadienones display rather short C=C bond lengths (1.276–1.292 Å at the MP2/6-31G* level), similar to that of C_3O_2 (1.279 Å, experimental estimate).[4e,f] For comparison, the experimental C=C bond length in ethylene, ketene, and propadienone are 1.339, 1.314, and 1.322 Å, respectively.[15] For the methyl (**4b**) and phenyl (**4c**) derivatives, strong delocalization of the π orbitals are predicted. The (Me)C–N and (Ph)C–N bond lengths (1.437 and 1.390 Å, respectively) are surprisingly short.

Charge Distributions. We have examined the charge distributions of the iminopropadienones using natural bond orbital (NBO) analysis[10] (MP2/6-31G*). As can be seen in Table 3, the NCCCO skeletons of all three iminopropadienones display an alternating charge distribution. It thus appears that the relatively short C=C bond lengths (1.276–1.292 Å) and the stabilities of the iminopropadienones may in part be due to strong electrostatic attraction. The large negative charge calculated for the terminal nitrogen atom suggests that an electron-withdrawing substituent will have a strong effect at the N terminus. The calculated dipole moments of **4a–c** at the MP2/6-31G* level are 3.02, 4.61, and 4.06 D, respectively. In view of their large dipole moments, the iminopropadienones are predicted to be significantly stabilized in solution. The charge distributions of these cumulenes also reveals that protonation at the central carbon (C_2) is highly favorable. This is readily confirmed by a recent combined experimental and theoretical study of protonated iminopropadienones.[16]

Stability of HNC_3O. To assess the stability of the unsubstituted iminopropadienone (**4a**), several fragmentation and rearrangement pathways have been examined. We have considered the dissociation reactions of **4a** to CO, HNC, HN, and H• (Table 4). The lowest energy fragmentation corresponding to the loss

TABLE 5: Calculated[a] IR Spectra of Iminopropadienones (RN=C=C=C=O) and Their Isotopomers

	wavenumber[b]				intensity[c]					wavenumber[b]				intensity[c]			
	RNC$_3$O		R^{15}N-C$_3$O[d]	RNC$_2$-^{13}CO[d]	RNC$_3$O		R^{15}N-C$_3$O[e]	RNC$_2$-^{13}CO[e]		RNC$_3$O		R^{15}N-C$_3$O[d]	RNC$_2$-^{13}CO[d]	RNC$_3$O		R^{15}N-C$_3$O[e]	RNC$_2$-^{13}CO[e]
	HF	MP2			HF	MP2				HF	MP2			HF	MP2		
HNC$_3$O (**4a**)																	
ν_1	3885	3695	−10	0	303	288	−10	1	ν_7	688	568	0	−16	72	30	0	−2
ν_2	2451	2446	−1	−30	4237	2538	−18	−55	ν_8	646	551	0	−11	57	16	1	−5
ν_3	2368	2204	−9	−30	1298	21	3	−20	ν_9	629	505	−1	−5	44	10	−1	4
ν_4	1760	1595	−12	−3	116	99	0	7	ν_{10}	523	498	−1	0	315	63	−3	0
ν_5	843	785	−10	−4	6	9	−2	1	ν_{11}	108	114	−1	0	4	3	0	0
ν_6	748	683	−4	0	578	647	1	0	ν_{12}	69	80	−1	0	4	0	0	0
CH$_3$NC$_3$O (**4b**)																	
ν_1	3313	3223	0	0	16	9	0	0	ν_{12}	1151	1086	−9	0	3	8	0	0
ν_2	3313	3197	0	0	16	10	0	0	ν_{13}	665	664	−5	−3	69	7	0	0
ν_3	3233	3108	0	0	40	50	0	1	ν_{14}	665	557	0	−15	69	22	0	0
ν_4	2568	2453	−3	−26	2023	3131	−47	−79	ν_{15}	657	541	0	−15	45	11	0	−2
ν_5	2434	2245	−15	−31	5062	22	11	−13	ν_{16}	603	509	−2	−1	66	59	−1	−1
ν_6	1849	1669	−16	−5	45	146	5	12	ν_{17}	603	457	−2	−1	66	31	−1	1
ν_7	1636	1557	0	0	6	6	0	0	ν_{18}	78	174	−2	0	1	41	−1	0
ν_8	1636	1548	0	0	6	6	0	0	ν_{19}	78	81	−1	0	1	0	0	0
ν_9	1602	1500	0	0	206	139	2	2	ν_{20}	42	76	0	0	7	4	0	0
ν_{10}	1260	1190	−2	0	1	59	0	0	ν_{21}	42	51	0	0	7	2	0	0
ν_{11}	1260	1155	−2	0	1	0	0	0									
PhNC$_3$O (**4c**)[f]																	
ν_1	3403	3228	0	0	4	7	0	0	ν_{22}	1091	923	0	0	2	0	0	0
ν_2	3399	3219	0	0	16	9	0	0	ν_{23}	1040	888	−7	−1	8	1	−1	0
ν_3	3390	3210	0	0	27	7	0	0	ν_{24}	972	869	0	0	19	2	0	0
ν_4	3378	3201	0	0	8	1	0	0	ν_{25}	947	819	0	0	0	0	0	0
ν_5	3368	3194	0	0	1	2	0	0	ν_{26}	853	738	0	0	78	108	0	0
ν_6	2532	2423	−4	−22	1978	4049	−82	−50	ν_{27}	762	694	−2	−1	19	16	1	−1
ν_7	2421	2205	−16	−32	8488	55	19	−53	ν_{28}	726	661	0	0	69	4	0	0
ν_8	1866	1643	−16	−7	176	352	29	28	ν_{29}	680	652	−1	0	1	6	−1	0
ν_9	1798	1594	0	0	74	50	−12	−5	ν_{30}	666	628	0	−12	69	40	−1	10
ν_{10}	1782	1579	0	0	6	9	0	0	ν_{31}	663	603	0	−15	69	33	0	9
ν_{11}	1660	1526	0	0	90	49	−5	−3	ν_{32}	604	589	−4	−6	58	41	−2	−10
ν_{12}	1619	1497	0	0	5	4	0	0	ν_{33}	600	572	−3	−2	49	18	1	−10
ν_{13}	1470	1389	0	0	0	1	0	0	ν_{34}	554	502	−1	0	7	5	0	0
ν_{14}	1333	1311	0	0	1	10	0	0	ν_{35}	457	437	−5	0	0	16	0	0
ν_{15}	1328	1245	0	0	52	2	0	0	ν_{36}	438	417	0	0	0	0	0	0
ν_{16}	1292	1241	0	0	2	0	0	0	ν_{37}	375	346	0	−2	2	9	0	0
ν_{17}	1215	1208	−1	0	1	75	5	0	ν_{38}	278	251	−3	0	0	0	0	0
ν_{18}	1184	1105	0	0	3	9	0	0	ν_{39}	92	90	0	0	1	6	0	0
ν_{19}	1128	1052	0	0	1	6	0	0	ν_{40}	63	71	−1	0	1	0	0	0
ν_{20}	1128	1023	0	0	0	0	0	0	ν_{41}	35	24	0	0	0	1	0	0
ν_{21}	1101	928	0	0	0	0	0	0	ν_{42}	11	18	0	0	0	1	0	0

[a] 6-31G* basis set, unless otherwise noted. [b] In cm^{-1}. [c] In km mol^{-1}. [d] Isotopomer wavenumber shifts (MP2 values). [e] Intensity changes due to isotopic substitutions (MP2 values). [f] 3-21G basis set at the MP2 level.

of CO is enthothermic by 330 kJ mol^{-1}. Loss of the hydrogen atom is also unfavorable (by 361 kJ mol^{-1}). Note that the product of the reaction **4a** → HNCC + CO, can rearrange to a more stable isomer, i.e., HCCN. However, the "nonlinear" dissociations to HCCN is also calculated to be endothermic (by 229 kJ mol^{-1}). The energy requirement for other dissociation reactions are significantly higher (Table 4). Hence, iminopropadienone (**4a**) is predicted to be a thermodynamically stable species. This finding is consistent with the experimental observation of HNC$_3$O by neutralization–reionization mass spectrometry.[2]

Cyanoketene (**9**) is calculated to be the global minimum on the C$_3$HNO potential energy surface. The iminopropadienone isomer (**4a**) lies 68 kJ mol^{-1} above **9**. Rearrangement of **4a** to **9** can, in theory, take place via a 1,3-hydrogen shift, involving a four-centre transition structure **10** (Figure 3). The barrier for this process is substantial, 402 kJ mol^{-1}, even larger than those required for the fragmentations **4a** to HNCC + CO and H$^\bullet$ + NCCCO$^\bullet$. There is strong experimental evidence that the tautomerization of iminopropadienone to cyanoketene in high temperature FVP experiments[2] occurs via wall collision or by intermolecular proton transfer.[3b]

Ionization Energy and Heat of Formation of HNC$_3$O. Adiabatic (IE$_a$) and vertical (IE$_v$) ionization energies of HNC$_3$O (**4a**) were calculated at the G2(MP2) level of theory, which in general can reproduce ionization energies to within 0.1 eV.[17] For the isoelectronic analogue C$_3$O$_2$, the calculated adiabatic ionization energy (10.54 eV) is in very good agreement with the experimental value (10.60 eV).[18] The predicted IE$_a$ and IE$_v$ values of iminopropadienone **4a** are 9.51 and 9.74 eV, respectively (Table 4). The large difference between IE$_a$ and IE$_v$ (0.23 eV) is attributed to the large change in molecular geometry upon ionization. The iminopropadienone radical cation is calculated to have a strongly bent structure (**11**, Figure 3), in contrast to the essentially linear structure of the corresponding neutral. The calculated central CCC angle of **11** is 128.5°, significantly smaller than the experimental ∠CCC value (156°) for carbon suboxide.[4b,c]

Two independent methods (I and II) were used to determine the heat of formation ($\Delta H_f°$) of HNC$_3$O (**4a**). In method I, $\Delta H_f°_{298}$ (HNC$_3$O) was evaluated from the theoretical energy change (−66 kJ mol^{-1} at 298 K)[19] for the isodesmic reaction (eq 1) together with accepted literature $\Delta H_f°_{298}$ values for formaldehyde (−109 kJ mol^{-1})[18] and carbon suboxide (−94 kJ mol^{-1}),[18] and a recently revised $\Delta H_f°_{298}$ value for formaldimine (86 kJ mol^{-1}).[20] The predicted $\Delta H_f°_{298}$ value for **4a** using method I is 167 kJ mol^{-1}. In method II, $\Delta H_f°$ was obtained from the calculated heat of atomization (eq 2)in conjunction with the

$$\mathrm{HN{=}C{=}C{=}C{=}O + CH_2{=}O \rightarrow O{=}C{=}C{=}C{=}O + CH_2{=}NH} \quad (1)$$

$$\mathrm{HN{=}C{=}C{=}C{=}O \rightarrow 3C + N + O + H} \quad (2)$$

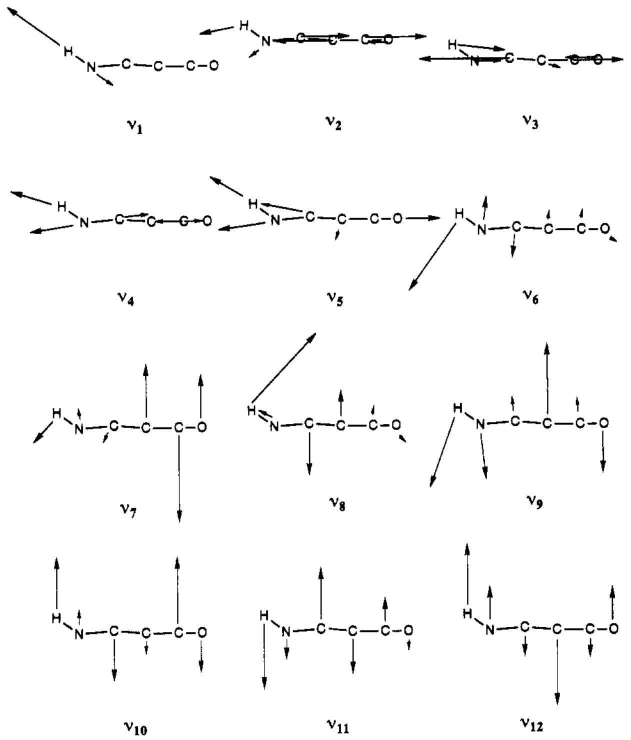

Figure 4. Calculated normal vibrations of HNC_3O (**4a**) at the MP2/6-31G* level. Vibrations ν_1–ν_9 are in the x,y plane (plane of paper), while vibrations ν_{10}–ν_{12} are in the x,z plane (out of the plane of paper).

TABLE 6: Calculated Wavenumbers (cm^{-1}) and IR Intensities (km mol^{-1}) of Cumulenic Stretching Vibrations of Iminopropadienones

	wavenumber		intensity	
	MP2/3-21G	MP2/6-31G*	MP2/3-21G	MP2/6-31G*
		HNC_3O (**4a**)		
ν_2	2434	2446	2066	2538
ν_3	2175	2204	2	21
		CH_3NC_3O (**4b**)		
ν_4	2432	2452	2668	3131
ν_5	2216	2244	15	22

TABLE 7: Comparison of Calculated Cumulenic CO Stretching Wavenumbers (cm^{-1}) with Experimental Values

molecule	theory[a]	experiment	ratio[b]
$O{=}C{=}O$	2448	2349[c]	0.96
$O{=}C{=}C{=}C{=}O$	2485	2290[c]	0.92
$CH_2{=}C{=}O$	2235	2152[c]	0.96
$CH_2{=}C{=}C{=}O$	2207	2125[d]	0.96
$CH_3N{=}C{=}C{=}C{=}O$	2453	2279[c]	0.93
$HN{=}C{=}C{=}C{=}O$	2446		

[a] MP2/6-31G* values. [b] Experiment value/calculated value. [c] From ref 23. [d] From ref 13. [e] From ref 1.

accurate heats of formation of atomic C, N, O, and H.[18] This leads to a $\Delta H_f°_{298}$ value of 175 kJ mol^{-1} for **4a**, reasonably close to the value computed by method I. Using a similar approach (method II), the G2(MP2) $\Delta H_f°_{298}$ for C_3O_2 is −98 kJ mol^{-1}, in excellent agreement with the experimental value of −94 kJ mol^{-1}.[18] Because of the uncertainty of $\Delta H_f°_{298}(CH_2NH)$ involved in method I, the method II value (175 kJ mol^{-1}) constitutes our final best theoretical estimate, to which an error bar of approximately 10 kJ mol^{-1} is to be associated.[17]

Vibrational Wavenumbers and Infrared Spectra. The infrared spectra of all three iminopropadienones (**4a–c**), calculated at the HF/6-31G* and MP2/6-31G* (MP2/3-21G for the phenyl derivative) levels are reported in Table 5. The normal vibrations calculated for the parent compound, HNC_3O (**4a**) at the MP2/6-31G* level are illustrated in Figure 4. As can be seen in Table 5, the characteristic features of the spectra of the iminopropadienones are the strong absorption bands of the cumulenic[21] $N{=}C{=}C{=}C{=}O$ stretching wavenumbers, ν_2 and ν_3 for **4a**, ν_4 and ν_5 for **4b**, and ν_6 and ν_7 for **4c**. In the first approximation, the two cumulenic vibrations can be considered as a mixing of the $N{=}C{=}C$ and $C{=}O$ vibrations. The higher-wavenumber "antisymmetric" ketenic[21] stretch is associated predominantly with the $C{=}C{=}O$ moiety, while the lower-wavenumber "symmetric" stretch has a higher proportion of $C{=}N$ vibration. At the Hartree–Fock level, both the antisymmetric and symmetric vibrations are predicted to yield strong absorptions, with the symmetric stretch considerably stronger than the antisymmetric stretch for **4b** and **4c**. Inclusion of electron correlation at the MP2 level leads to a drastic change in the relative intensities of the two cumulenic vibrations. In fact, the symmetric cumulenic stretch (e.g., ν_3 in **4a**) becomes a very weak band at the MP2 level. Since MP2 wavenumber calculation employing the 6-31G* basis set was not feasible for the phenyl derivative (**4c**), a smaller 3-21G basis set was used instead. To assess the likely accuracy of the MP2/3-21G level, we have determined also the IR spectra of **4a** and **4b** at the MP2/3-21G level. As can be seen in Table 6, the calculated MP2/3-21G harmonic wavenumbers of the cumulenic stretches are reasonably close to the MP2/6-31G* values. More importantly, the relative intensities are essentially the same as when using the larger 6-31G* basis set. This lends confidence to our prediction of the IR intensities for the phenyl derivative (**4c**). Indeed, the calculated MP2 relative intensities of ν_6 and ν_7 for **4a** is in excellent accord with the experimental observations, as described in section 3. Hence, *inclusion of electron correlation is essential for the correct prediction of relative intensities of the cumulenic stretching wavenumbers of iminopropadienones*. Significant wavenumber shifts are observed for these vibrations when going from R = H to R = CH_3 to R = Ph (Table 5).

To provide a more definitive assignment of the vibrational spectra of the iminopropadienones (**4a–c**), the calculated IR spectra of the ^{15}N ($R^{15}NCCCO$) and ^{13}C($RNCC^{13}CO$) isotopomers are reported in Table 5. Significant wavenumber shifts of the cumulenic bands are predicted for the ^{15}N and ^{13}C isotopomers for all three cumulenes. The shifts calculated for the ^{13}C isotopomers are larger than those for the ^{15}N isotopomers. Enormous intensity changes are calculated for the symmetric cumulenic stretches (the smaller peaks) of the ^{13}C isotopomers. For the methyl derivative of iminopropadienone (**4b**), the intensity of the ν_5 vibration is calculated to decrease by 60%, while for the parent compound (ν_3 in **4a**) and the phenyl derivative (ν_7 in **4c**), the symmetric cumulenic band is predicted to almost disappear in their ^{13}C spectra.

As pointed out in the structure section, the iminopropadienones are predicted to be "flexible" molecules. This is readily confirmed by the existence of some very low-wavenumber vibrations. In particular, we note the chain-bending vibrations, e.g., ν_{11} in **4a** (Table 5 and Figure 4). It is noteworthy that the three lowest bending fundamentals of HNCO are severely perturbed by Coriolis mixing.[14] Likewise, the importance of including the Coriolis coupling term to describe the bending δ_{NS} of N_2S has been reported.[22] Hence, the six frequencies in **4a** lying between 500 and 850 cm^{-1} (ν_5–ν_{10}) may require Coriolis correction for reliable theoretical prediction.

Finally, we have determined the CO stretching wavenumbers of several molecules containing a cumulenic CO moiety at the MP2/6-31G* level (Table 7). There is excellent agreement between theory and experiment.[23] The calculated cumulenic CO stretching wavenumbers are 4–8% larger than the experimental values and suggest a scaling factor of 0.94 may be appropriate for the cumulenic stretching wavenumbers of the unsubstituted iminopropadienone (**4a**). Thus, our predicted values of the cumulenic vibrations ν_2 and ν_3 of **4a** are 2299 and 2072 cm^{-1}, respectively.

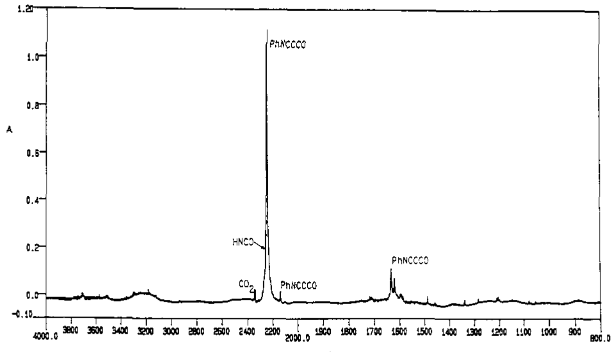

Figure 5. Ar matrix IR spectrum (12 K) of $PhNC_3O$ (**4c**), generated by FVP of **1** at 800 °C.

TABLE 8: Experimental IR Spectra[a] of PhN=C=C=C=O (4c) and Its Isotopomers (Ar Matrix, 12 K)

$PhNC_3O$[b]	$Ph^{15}NC_3O$	$PhNC_2{}^{13}CO$
2247 vs (2253)	2247 vs	2222 vs
2141 w (2154)	2126 w	
1633 m (1661)	1623 m	1630 m
1620 m (1600)	1608 m	1617 m
1490 w (1478)	1490 w	1490 w
1284 w (1308)	1284 w	1284 w
1210 w (1182)	1208 w	1210 w
754 w (759)	754 w	
685 w (678)	685 w	
565 w (589)	565 w	

[a] Wavenumbers in cm^{-1}. [b] HF/6-31G* values (scaled by a factor of 0.89)[8] are in parentheses.

3. Experimental IR Spectra of $PhNC_3O$ and Its Isotopomers

The Ar matrix IR spectrum of the phenyl derivative (**4c**), generated by FVP of **1c** at 800 °C, is shown in Figure 5.[24] The same spectrum is obtained from **2c** and **3c** except that CO_2 and acetone together with dimethylamine or methanethiol will, of course, also be seen in the latter spectra. By far the most prominent feature is the very strong band at 2247 cm^{-1}. As shown below, the very weak band at 2141 cm^{-1} is also due to the cumulenic moiety in PhN=C=C=C=O. Since the calculated Hartree–Fock wavenumbers generally exceed the experimental values by 12%,[8] a scaling factor of 0.89 has been applied to the calculated harmonic wavenumbers at the HF/6-31G* level. The scaled calculated values are in excellent accord with the observed IR wavenumbers of **4c** (Table 8).

The ^{15}N and ^{13}C labeled cumulenes **6** and **8** were generated by FVP of the Meldrum's acid derivatives **5** and **7**, respectively (see Experimental Section for the syntheses). The infrared spectrum of **6** reveals a significant shift of the small peak at 2141 cm^{-1}, whereas the major peak at 2247 cm^{-1} is hardly affected (Figure 6 and Table 8). In contrast, the ^{13}C-labeled compound **8** shows a large shift of the ketenic band at 2247 cm^{-1}, while the small peak at 2141 cm^{-1} virtually disappears (Figure 6 and Table 8).

These observations are nicely confirmed by the calculations at the MP2/3-21G level (Table 5). While both vibrations in the cumulene region (ν_6 and ν_7) involve all the cumulated atoms, ν_7 (the "symmetric" cumulenic vibration) is dominated by the C=N stretching. As a consequence, the band ν_7 is strongly affected by ^{15}N labeling in **4c** (2141–2126 cm^{-1}). The theoretical calculations reproduce the experimental isotopic shifts almost quantitatively (16 cm^{-1} for ν_7 and 4 cm^{-1} for ν_6 in **6**). ^{13}C labeling as in **8** is calculated to have a large effect on both ν_6 and ν_7 (22 and 32 cm^{-1}, respectively). The computed isotopic shift for ν_6 is in good accord with the measured value (25 cm^{-1}). Most importantly, the calculated intensity of ν_7 *decreases* 30-fold in **8**, thereby explaining the virtual disappearance of this band in the experimental spectrum (Figure 6 and Table 8).

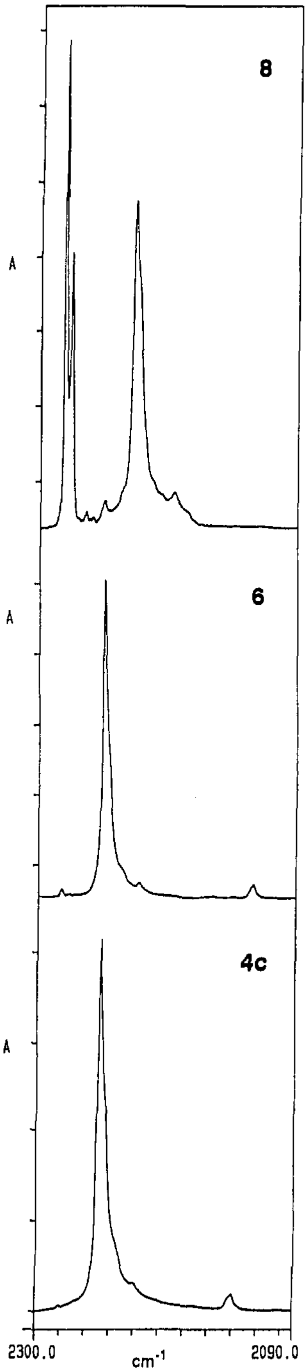

Figure 6. Partial IR spectra of **4c**, **6**, and **8** (Ar, 12 K). The cumulenic signals at 2247 and 2141 cm^{-1} (**4c**), 2247 and 2126 cm^{-1} (**6**), and 2222 cm^{-1} (**8**) are shown. The strong signals near 2278 and 2273 cm^{-1} in the spectrum of **8** are due to $^{13}CO_2$.

4. Conclusion

The iminopropadienones, RN=C=C=C=O (R = H, CH_3, and Ph) are predicted to have an almost linear NCCCO backone (∠CCC ≈ 176°). The calculated CCC bending potential, however, is extremely flat. The very good agreement between the calculated and experimental IR spectra of $PhNC_3O$ (**4a**) and its ^{15}N and ^{13}C isotopomers, **6** and **8**, strongly supports the identification of these compounds based largely on chemical and mass spectrometric evidence.[1,2] This also gives cause to believe that the calculated structures of iminopropadienones are close to reality. The calculated stability of HNC_3O is consistent with its experimental observation in the gas phase.[2] We are currently extending this fruitful interplay between theory and experiment to the characterization of bisimines RN=C=C=C=NR′.[3]

5. Experimental Section

Apparatus and cryostats used for flash vacuum pyrolyses were as previously described.[25] IR spectra were recorded on a Perkin-Elmer 1720X FTIR spectrometer at a resolution of 1 cm^{-1}.

Materials. Aniline[^{15}N] (99 atom % ^{15}N) and barium carbonate[^{13}C] (>90 atom % ^{13}C) were obtained from Cambridge Isotope Laboratories, Woburn, MA.

2,2-Dimethyl-5-[dimethylamino([^{15}N]phenylamino)methylene]-1,3-dioxane-4,6-dione (5) was synthesized from 2,2-dimethyl-5-[bis(imethylthio)methylene]-1,3-dioxane-4,6-dione (0.263 g; 1.06 mmol) in 5 mL of EtOH by adapting the method published for the unlabeled compound[1] with aniline[^{15}N] (0.100 g; 1.06 mmol) under reflux for 2 h. The solvent was removed at 15 Torr (25 °C). THF (10 mL) was added, followed by 0.5 mL of 40% aqueous dimethylamine and 287 mg (1.06 mmol) of $HgCl_2$. The mixture was stirred for 30 min at 25 °C, filtered; and the clear filtrate was extracted with CH_2Cl_2 (13 × 10 mL). The organic layer was washed with H_2O (2 × 5 mL), dried over Na_2SO_4, filtered, and concentrated at 17 Torr (25 °C). The resulting solid (0.24 g; 77%) was recrystallized from THF/pentane to give the colorless compound, mp 192–194 °C; ^1H NMR δ 1.71 (s, 6 H; 2 CH_3), 2.92 (s, 6 H; $N(CH_3)_2$), 7.1–7.4 (M, 5H; aromatic), 9.13 (s, 1 H; NH); ^{13}C NMR (DMSO-d_6) δ 26.26 ($C(CH_3)_2$), 39 ($N(CH_3)_2$), 72.37 (*C*-5), 100.80 (*C*-2), 123.00 (phenyl-ortho), 125.00 (phenyl-para), 128.60 (d, $J_{^{15}N}$ = 1.4 Hz; phenyl-meta), 139.53 (d, $J_{^{15}N}$ = 15.8 H z; phenyl-*C*1) 161.76 (*C*O), 162.91 (d, $J_{^{15}N}$ = 19.0 Hz; ^{15}N–*C*–N).

2,2-Dimethyl-5-[dimethylamino(phenylamino)methylene]-1,3-dioxane-4,6-dione-$^{13}C_2$ (7). Barium carbonate[^{13}C] was converted to $^{13}CO_2$ using a published procedure.[26] $^{13}CO_2$ was converted into malonic acid[1,3-$^{13}C_2$] and then into the doubly labeled Meldrum's acid (2,2-dimethyl-1,3-dioxane-4,6-dione[4,6-$^{13}C_2$]) using literature methods.[27] The Meldrum's acid was converted to the 5-[bis(imethylthio)methylene] derivative using the standard method,[28] and the title compound **7** was then prepared in the same way as the unlabeled compound[1] and as described for the ^{15}N-labeled analogue (**6**) above. Mp 192–194 °C; ^1H NMR ($CDCl_3$) δ 1.61 (s, 6 H; $(CH_3)_2C$), 2.86 (s, 6 H; $N(CH_3)_2$), 7.0–7.3 (m, 5 H; aromatic), 9.27 (br s, 1 H; NH); ^{13}C NMR ($CDCl_3$) δ 26.30 ($(CH_3)_2C$), 41.67 ($N(CH_3)_2$), 72.15 (*C*-5), 102.78 (*C*-2), 122.86 (phenyl-ortho), 125.99 (phenyl-para), 129.47 (phenyl-meta), 138.83 (phenyl-*C*1), 164.3 (*C*O), 166.7 (N*C*N).

General Procedure for Flash Vacuum Pyrolysis. The Meldrum's acid precursor (10–15 mg, 0.03–0.05 mmol) was gently sublimed (80–100 °C) with a continuous stream of Ar ((6–8) × 10^{-5} mbar; 50 mbar of Ar in 15 min) into the pyrolysis apparatus[25] (10-cm quartz tube; 8-mm i.d. 500 °C). The product was collected on a BaF_2 (or KBr) disk at 16–18 K and FTIR spectra were recorded periodically to monitor the formation of the matrix. A typical pyrolysis/deposition took 3 h to completion. Reference spectra of the starting materials, acetone, and dimethylamine were obtained under similar conditions, without pyrolysis.

Acknowledgment. We are grateful for financial support of this research by the Australian Research Council (ARC). T.M. and S.S. would like to thank the Deutsche Forschungsgemeinschaft for postdoctoral fellowships. M.W.W. thanks the ARC for the award of an Australian Research Fellowship. We thank Dr. Douglas Brecknell and Dr. Regis Leung-Toung for technical assistance, and the University of Queensland and the Queensland Supercomputing Laboratories for generous allocations of computing time.

References and Notes

(1) Mosandl, T.; Kappe, C. O.; Flammang, R.; Wentrup, C. *J. Chem. Soc., Chem. Commun.* **1992**, 1571.

(2) Flammang, R.; Laurent, S.; Flammang-Barbieux, L.; Wentrup, C. *Rapid. Commun. Mass Spectrom.* **1992**, *6*, 667.

(3) (a) Stadtmüller, S.; White, R.; Flammang, R.; Laurent, S.; Wong, M. W.; Wentrup, C. To be published. (b) Flammang, R.; Laurent, S.; Flammang-Barbieux, M.; Wentrup, C. *Org. Mass Spectrom.* **1993**, *28*, 1161.

(4) (a) Kappe, T. *Angew. Chem., Int. Ed. Engl.* **1974**, *13*, 491. (b) Jensen, P.; Johns, J. W. C. *J. Mol. Spectrosc.* **1986**, *118*, 248. (c) Jensen, P. *J. Mol. Spectrosc.* **1984**, *104*, 59. (d) Loses, R. L.; Sabin, J. R.; Oddershede, J. *J. Mol. Spectrosc.* **1981**, *86*, 357. (e) Bunker, P. R. *J. Mol. Spectrosc.* **1980**, *80*, 422. (f) Webber, W. H. *J. Mol. Spectrosc.* **1980**, *79*, 396. (g) Duckett, J. A.; Mills, I. M.; Robiette, A. G. *J. Mol. Spectrosc.* **1976**, *63*, 249. (h) Smith, W. M.; Leroy, G. E. *J. Chem. Phys.* **1966**, *45*, 1767.

(5) Hehre, W. J.; Radom, L.; Schleyer, P. v. R.; Pople, J. A. *Ab Initio Molecular Orbital Theory*; Wiley: New York, 1986.

(6) Frisch, M. J.; Trucks, G. W.; Head-Gordon, M.; Gill, P. M. W.; Wong, M. W.; Foresman, J. B.; Johnson, B. G.; Schlegel, H. B.; Robb, M. A.; Replogle, E. S.; Gomperts, R.; Andres, J. L.; Raghavachari, K.; Binkley, J. S.; Gonzalez, C.; Martin, R. L.; Fox, D. J.; DeFrees, D. J.; Baker, J.; Stewart, J. J. P.; Pople, J. A. *GAUSSIAN 92*; Gaussian Inc.: Pittsburgh PA, 1992.

(7) (a) Handy, N. C.; Amos, R. D.; Gaw, J. F.; Rice, J. E.; Simandiras, E. D. *Chem. Phys. Lett.* **1985**, *120*, 151. (b) Pople, J. A.; Krishnan, R.; Schlegel, H. B.; Binkley, J. S. *Int. J. Quantum Chem. Symp.* **1979**, *13*, 225.

(8) (a) Pople, J. A.; Scott, A. P.; Wong, M. W.; Radom, L. *Isr. J. Chem.*, in press. (b) Pople, J. A.; Schlegel, H. B.; Raghavachari, K.; DeFrees, D. J.; Binkley, J. S.; Frisch, M. J.; Whitesides, R. F.; Hout, R. F.; Hehre, W. J. *Int. J. Quantum Chem. Symp.* **1981**, *15*, 269.

(9) (a) Curtiss, L. A.; Raghavachari, K.; Pople, J. A. *J. Chem. Phys.* **1993**, *98*, 1293. (b) Curtiss, L. A.; Raghavachari, K.; Trucks, G. W.; Pople, J. A. *J. Chem. Phys.* **1991**, *94*, 7221.

(10) (a) Glendening, E. D.; Reed, A. E.; Carpenter, J. E.; Weinhold, F. NBO Version 3.1. For reviews, see (b) Reed, A. E.; Curtiss, L. A.; Weinhlod, F. *Chem. Rev.* **1988**, *88*, 899. (c) Weinhlod, F.; Carpenter, J. E. In *The Structure of Small Molecules and Ions*; Naaman, R., Vager, Z., Eds.; Plenum: New York, 1988.

(11) Pople, J. A.; Head-Gordon, M.; Raghavachari, K. *J. Chem. Phys.* **1987**, *87*, 5968.

(12) (a) Scott, A. P.; Radom, L. *Chem. Phys. Lett.* **1992**, *200*, 15. (b) Farnell, L.; Radom, L. *J. Am. Chem. Soc.* **1984**, *106*, 25. (c) Farnell, L.; Radom, L. *Chem. Phys. Lett.* **1982**, *91*, 373. (d) Taylor, P. R. *J. Comput. Chem.* **1984**, *6*, 589. (e) Brown, R. D.; Godfrey, P. D.; Ball, M. J.; Godfrey, S.; McNaughton, D.; Rodler, M.; Kleibomer, B.; Champion, R. *J. Am. Chem. Soc.* **1986**, *108*, 6534.

(13) Chapman, O. L.; Miller, M. D.; Pitzenberger, S. M. *J. Am. Chem. Soc.* **1987**, *109*, 6867.

(14) East, A. L.; Johnson, C. S.; Allen, W. D. *J. Chem. Phys.* **1993**, *98*, 1299.

(15) Harmony, M. D.; Laurie, V. W.; Kuczkowski, R. L.; Schwendeman, R. H.; Ramsay, D. A.; Lovas, F. L.; Lafferty, W. J.; Maki, A. G. *J. Phys. Chem. Ref. Data* **1979**, *8*, 619.

(16) Flammang, R.; van Haverbeke, Y.; Wong, M. W.; Rühmann, A.; Wentrup, C. *J. Phys. Chem.*, submitted.

(17) Wong, M. W.; Radom, L. To be published.

(18) Lias, S. G.; Bartmess, J. E.; Liebman, J. F.; Holmes, J. L.; Levin, R. D.; Mallard, W. G. *J. Phys. Chem. Ref. Data* **1988**, *17*, Suppl. 1.

(19) The G2(MP2) H_{298} energies of HNC_3O, C_3O_2, CH_2CO and CH_2-NH are −244.442 36, −264.342 48, −114.332 26, and −94.457 26 hartrees, respectively.

(20) Smith, B. J.; Pople, J. A.; Curtiss, L. A.; Radom, L. *Aust. J. Chem.* **1992**, *45*, 285.

(21) In this paper, the term "ketenic" denotes the $C{=}C{=}O$ moiety while "cumulenic" refers to the whole cumulene skeleton including the CCO moiety.

(22) Collins, C. L.; Yamaguchi, Y.; Schaefer, H. F. *J. Chem. Phys.* **1993**, *98*, 4777.

(23) (a) Shimanouchi, T. *Tables of Molecular Vibrational Frequencies I*; Publication NSRDS-NBS 39; National Bureau of Standards, Washington, D.C. (b) Shimanouchi, T. *J. Phys. Chem. Ref. Data.* **1977**, *6*, 993.

(24) It is not necessary to isolate **4a** in an Ar matrix. It can be observed spectroscopically up to room temperature for brief periods of time.

(25) Wentrup, C.; Blanch, R.; Briel, H.; Gross, G. *J. Am. Chem. Soc.* **1988**, *110*, 1874.

(26) Mayor, C.; Wentrup, C. *J. Am. Chem. Soc.* **1975**, *97*, 7467.

(27) (a) Thies, H.; Franke, W.; Schwarz, H. *Synthesis* **1982**, 587. (b) Brown, R. F. C.; Browne, N. R.; Coulston, K. J.; Eastwood, F. W.; Irvine, M. J.; Pullin, D. E.; Wiersum, U. E. *Aust. J. Chem.* **1989**, *42*, 1321.

(28) Ye, F.-C.; Chen, B.-C.; Huang, X. *Syntheses* **1989**, 317. (b) Huang, X.; Chen, B.-C. *Ibid.* **1986**, 967. (c) Ben Cheikh, A.; Chuche, J.; Manisse, N.; Pommelet, J. C.; Netsch, K.-P.; Lorencak, P.; Wentrup, C. *J. Org. Chem.* **1991**, *56*, 970.